Myosin-II-Mediated Directional Migration of *Dictyostelium* Cells in Response to Cyclic Stretching of Substratum

Yoshiaki Iwadate,[†‡*] Chika Okimura,[†] Katsuya Sato,[§] Yuta Nakashima,[¶] Masatsune Tsujioka,[||††] and Kazuyuki Minami[¶]

[†]Department of Functional Molecular Biology, Graduate School of Medicine, Yamaguchi University, Yamaguchi, Japan; [‡]PRESTO, Japan Science and Technology Agency, Saitama, Japan; [§]Department of Mechanical Engineering, Faculty of Engineering,The University of Tokushima, Tokushima, Japan; [¶]Graduate School of Science and Engineering, Yamaguchi University, Yamaguchi, Japan; [||]Department of Biological Science, Graduate School of Science, Osaka University, Toyonaka, Osaka, Japan; and [††]Core Research for Evolutional Science and Technology Agency, Suita, Osaka, Japan

ABSTRACT Living cells are constantly subjected to various mechanical stimulations, such as shear flow, osmotic pressure, and hardness of substratum. They must sense the mechanical aspects of their environment and respond appropriately for proper cell function. Cells adhering to substrata must receive and respond to mechanical stimuli from the substrata to decide their shape and/or migrating direction. In response to cyclic stretching of the elastic substratum, intracellular stress fibers in fibroblasts and endothelial, osteosarcoma, and smooth muscle cells are rearranged perpendicular to the stretching direction, and the shape of those cells becomes extended in this new direction. In the case of migrating *Dictyostelium* cells, cyclic stretching regulates the direction of migration, and not the shape, of the cell. The cells migrate in a direction perpendicular to that of the stretching. However, the molecular mechanisms that induce the directional migration remain unknown. Here, using a microstretching device, we recorded green fluorescent protein (GFP)-myosin-II dynamics in *Dictyostelium* cells on an elastic substratum under cyclic stretching. Repeated stretching induced myosin II localization equally on both stretching sides in the cells. Although myosin-II-null cells migrated randomly, myosin-II-null cells expressing a variant of myosin II that cannot hydrolyze ATP migrated perpendicular to the stretching. These results indicate that *Dictyostelium* cells accumulate myosin II at the portion of the cell where a large strain is received and migrate in a direction other than that of the portion where myosin II accumulated. This polarity generation for migration does not require the contraction of actomyosin.

INTRODUCTION

Living cells are constantly subjected to a wide variety of mechanical stimulations, such as shear flow and substratum strain. They must sense the mechanical aspects of their environment and respond appropriately for proper cell function. For example, in vascular endothelial cells, blood shear flow activates various cell functions, such as gene expression, proliferation, and apoptosis (1). In the auditory hair cells of vertebrates, stereovillus deflections open mechanoelectrical transduction channels and cause changes in the membrane potential (2).

In general, cells adhere to the substratum via focal adhesion sites. Thus, it seems that the cells receive mechanical stimuli mainly from substrata in physiological conditions (3,4). To mimic this situation, one of the most appropriate techniques for applying mechanical stimuli artificially is to stretch the elastic substratum to which cells adhere (5–8). In response to the cyclic stretching of the elastic substratum, intracellular stress fibers in fibroblasts and in endothelial, osteosarcoma, and smooth muscle cells are rearranged perpendicular to the stretching direction, and the shape of the cells becomes extended in that direction (9–15). On the other hand, in the case of fast-crawling cell migration, we found that *Dictyostelium* cells migrate perpendicular to the cyclic stretching (16). However, the molecular mechanisms by which cyclic stretching induces directional migration in *Dictyostelium* cells remain unknown. Under total internal reflection fluorescence microscopy, *Dictyostelium* cells show a dense meshwork of actin filaments instead of stress fibers (17,18). Thus, the reaction of *Dictyostelium* cells to cyclic stretching should be different from those of fibroblasts and endothelial, osteosarcoma, and smooth muscle cells.

It is now generally believed that extension of the leading edge induced by actin polymerization (19,20) and retraction of the rear by contraction through myosin-II-dependent processes (21,22) are the driving forces of cell-crawling migration. If cells decide on their migrating direction in response to cyclic stretching of the substratum, the dynamics of actin and/or myosin II, and not the rearrangement of stress fibers, should be directly or indirectly regulated by the stimulation. In response to stretching of the cell surface by using a micropipette to suck it, myosin II localizes to the tip of the sucked cell lobe (23,24), indicating that the localization of myosin II is regulated by mechanical forces. Moreover, myosin-II-null cells cannot suppress lateral extrapseudopodia (25,26). Their path linearity and migration speed are significantly lower than those of wild-type cells under chemotactic conditions (27,28). Thus, myosin II is a possible candidate for

Submitted February 27, 2012, and accepted for publication January 7, 2013.

*Correspondence: iwadate@yamaguchi-u.ac.jp

Editor: Shin'ichi Ishiwata.

0006-3495/13/02/0748/11 $2.00

http://dx.doi.org/10.1016/j.bpj.2013.01.005

mediator of directional migration induced by mechanical forces.

In this study, cyclic stretching of the elastic substratum induced myosin II localization equally at both stretching sides in the cell. Wild-type cells migrated perpendicular to the stretching, whereas myosin-II-null cells migrated randomly. However, myosin-II-null cells expressing a myosin II variant that cannot hydrolyze ATP showed directional migration like that of wild-type cells. These results indicate that freely migrating *Dictyostelium* cells respond to the forces from the substratum, accumulating myosin II at the portion where a large strain is received and then migrating in a direction different from that in the portion where myosin II accumulated. This polarity generation for migration does not require the contraction of actomyosin.

MATERIALS AND METHODS

Cell lines

Dictyostelium discoideum cells were developed in Bonner's standard saline (10 mM NaCl, 10 mM KCl, and 3 mM $CaCl_2$) until they became aggregation-competent, as described previously (29). The *Dictyostelium* cell lines used were AX2 cells (referred to as wild-type cells but actually an axenic derivative of the wild-type strain NC4); AX2 cells expressing GFP-ABD120k; myosin II heavy-chain-null (*mhcA*$^-$) cells; *mhcA*$^-$ cells expressing GFP-myosin II, GFP-3xALA myosin II, GFP-3xASP myosin II, or GFP-E476K myosin II; and SibA-null (*SibA*$^-$) cells. ABD120k is the actin-binding domain of the actin-crosslinking protein ABP120 (30) and can only bind to filamentous actin. Fluorescence imaging of GFP-ABD120k reflects the distribution of filamentous actin. The gene encoding GFP-ABD120k was kindly provided by D. A. Knecht (University of Connecticut, Storrs, CT). This fusion gene was inserted into the pBIG expression vector by T. Q. Uyeda (National Institute of Advanced Industrial Science and Technology, Tokyo, Japan). In *Dictyostelium*, bipolar thick filament formation of myosin II is regulated by the phosphorylation of three threonine residues in the tail region (31). In the 3xALA cell line, the three threonine phosphorylation sites of myosin II heavy chain are replaced with alanine so that it mimics the constitutively unphosphorylated state and constitutively forms bipolar thick filaments. In 3xASP, the three threonine phosphorylation sites are replaced with aspartate residues, so that it mimics the constitutively phosphorylated state and cannot form thick filaments. E476K-mutant myosin II cannot hydrolyze ATP in *mhcA*$^-$ cells (32,33). SibA protein, similar to integrin beta, acts as an adhesion molecule in *Dictyostelium* (34). The *sibA* gene was disrupted using a knockout construct in which a 2-kb fragment (nucleotides 1205–3261) and a 1.4-kb fragment (nucleotides 4146–5529) of the coding region were inserted into pBlueScript II SK+ (Stratagene, La Jolla, CA) as a XbaI/BamHI and a KpnI fragment, respectively (35). Subsequently, a 1.9-kb hygromycin cassette was inserted between these fragments as a SalI fragment.

Cyclic stretching of substratum to record migrating trajectory of cells

Stretching of the substratum was performed according to the methods described previously (16). Briefly, elastic sheets, 22 mm × 40 mm, were made from polydimethylsiloxane (Sylgard 184, Dow Corning Toray, Tokyo, Japan). One 22-mm side of the sheet was fixed and the other connected to a coiled shape-memory alloy (BioMetal Helix150, Toki, Gifu, Japan). Sequential square voltage pulses were applied to the coiled SMA, which induced cyclic stretching and relaxation of the sheet. In all experiments, the stretching ratio, time cycle, and duty ratio of stretching and relaxation were adjusted to 20%, 5 s, and 1:1, respectively, by modulating the frequency and the duty ratio of the square voltage pulses. Using elastic sheets, it is impossible to exclude the Poisson effect completely. When the sheet was stretched, perpendicular shrinkage of ~5% took place simultaneously. Cells show random migration under the cyclic stretching stimulus of a 10% stretching ratio, indicating that cyclic stretching of $<10\%$ does not affect the directionality of cell migration (16). Thus, in all experiments in this study, the perpendicular shrinkage should not affect the directionality of cell migration (see Iwagate and Yumura (16) for details).

Statistical analysis of migrating trajectory of cells under cyclic stretching

Migrating cells on a substratum under cyclic stretching were observed under phase-contrast microscopy using an inverted microscope (TS100, Nikon, Tokyo, Japan) with a 20× objective lens (LWD ADL 20xF, Nikon). Images taken by a CMOS camera (DMK41BUC02, Argo, Osaka, Japan) were transferred to a PC at 30-s intervals for 30 min and analyzed using ImageJ Ver. 1.42 with two plug-ins, Manual Tracking and a Chemotaxis and Migration tool. In this analysis, the angle (θ) between the horizontal line and a straight line that connected the starting and ending points of a migrating cell (see Fig. 3 *A*, *inset*) was measured. As an index of the directional migration, $|\sin\theta|$ was calculated. When all cells migrate parallel to the stretching direction under cyclic stretching (0°–180°), the average $|\sin\theta|$ should be 0, whereas when cells migrate perpendicular to the stretching direction (90°–270°), the value should be 1. When cells migrate equally in all directions, the value should be $2/\pi = 0.64$. In preparing histograms, as shown in Figs. 3, 4, and 7, the interior angle of each datum was 66.0°. This means that, for example, the value of the cells at 90° includes the number of cells that migrated in the direction from 57° to 123°. Directionality was also calculated. It is expressed as the linear distance between the start and end points of migration for 30 min divided by the pathlength of the trajectory between the same points. When a cell migrates on a straight path, the value should be 1. On the other hand, when it migrates windingly, the value should be smaller. Statistical analysis was performed by two-tailed Student's *t*-test.

Analysis of the relationship between pseudopod dynamics and myosin II localization in free migrating cells without stretching of substratum

The migrating *mhcA*$^-$ cells expressing GFP-myosin II or GFP-E476K myosin II on a coverslip were observed with an inverted microscope (Ti, Nikon) equipped with a laser confocal scanner unit (CSU-X1, Yokogawa, Tokyo, Japan) with a 100× objective lens (CFI Apo TIRF 100xH/1.49, Nikon). The fluorescence images were detected with an EM CCD camera (DU897; Andor, Belfast, Northern Ireland).

Two images taken at a time interval of 40 s were arbitrarily picked up from the sequential images (Fig. 1, *A* and *B*). In the first image (Fig. 1 *A*, $t = t_0$), a dotted line was drawn from the centroid to a point on the boundary of a cell. On the dotted line, the distance from the centroid to the point was defined as l_1. The maximum value of GFP fluorescence in the intersection (Fig. 1 *A*, *black bar*) of the dotted line and the area 2 μm from the cell boundary (Fig. 1 *A*, *orbital gray area*) was defined as *F*. In the second image (Fig. 1 *B*, $t = t_0 + 40$ s), a dotted line was drawn from the centroid at $t = t_0$, not $t = t_0 + 40$ s, in the same direction as in the first image. The distance between the centroid at $t = t_0$ and the cell boundary was defined as l_2. *F* and l_2/l_1 were calculated along the 12 dotted

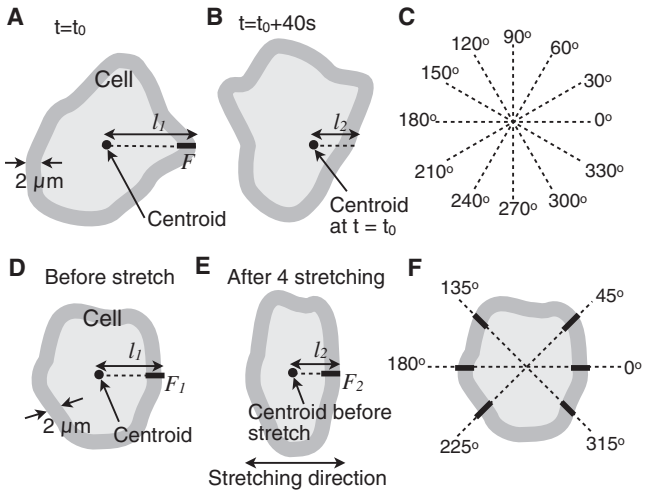

FIGURE 1 Estimation of myosin II-localization and pseudopod dynamics that follow. (*A–C*) From two sequential images at a time the interval of 40 s, l_1, l_2 and F were defined as shown in *A* and *B* (see Materials and Methods for details). F and l_2/l_1 were calculated along the 12 dotted lines in *C*. F refers to spontaneous localization of myosin II in freely migrating cells. The value l_2/l_1 means the contraction or expansion of pseudopodia. (*D–F*) From two images before and after four repeats of stretching using the device shown in Fig. 2 *A*, l_1, l_2, F_1 and F_2 were defined as shown in *D* and *E* (see Materials and Methods for details). The values l_1, l_2, F_1 and F_2 were calculated along the six dotted lines in *F*. F_2/F_1 means localization of myosin II in response to the four repeats of stretching of substratum.

lines in Fig. 1 *C*) at intervals of 30°. When the pseudopod expands, l_2/l_1 should be >1.

Cyclic stretching of substratum for observation of GFP-myosin II

The stretching device described in the above section was optimized for observation of the migrating trajectory with a low-power objective lens. To observe the intracellular localization of GFP-myosin II in response to the stretching of the substratum, a fine microstretching device (Fig. 2 *A*) was used (see Sato et al. (36) for a detailed description of the device). Briefly, an elastic microchamber was made from polydimethylsiloxane (KE-106, Shin-Etsu Chemical, Tokyo, Japan). A chamber stretching linkage mechanism was made from photoresist (SU-8, Microchem, Westborough, MA) and fabricated with a photolithography technique. Cells were plated onto the elastic thin substratum, 100 μm × 400 μm, $t = 10$ μm, in the microchamber. Strain distribution on the thin substratum was evaluated as previously described. In the test, the magnitude of stretch in the entire microchamber was 0.26 (26% stretch). The results for strain distribution measurements are indicated in Fig. 2 *B*. There was a roughly homogeneous strain field. Strain in rectangular axis to stretch was well suppressed by the support flame of the microchamber. There was only 0.8% compressing strain in the rectangular axis to stretch. The migrating *mhcA*$^-$ cells expressing GFP-myosin II in the chamber of the device were observed with an inverted microscope (Ti, Nikon) equipped with a laser confocal scanner unit (CSU-X1, Yokogawa) with a 100× objective lens (CFI Apo TIRF 100xH/1.49, Nikon). The fluorescence images were detected with an EM CCD camera (DU897, Andor). The chamber (Fig. 2 *A*) was stretched 20% in length in the linear direction by pushing the bottom part of the device with a glass microneedle (Fig. 2 *A*) connected to a piezo actuator (MC-140L, MESS-TEC, Saitama, Japan).

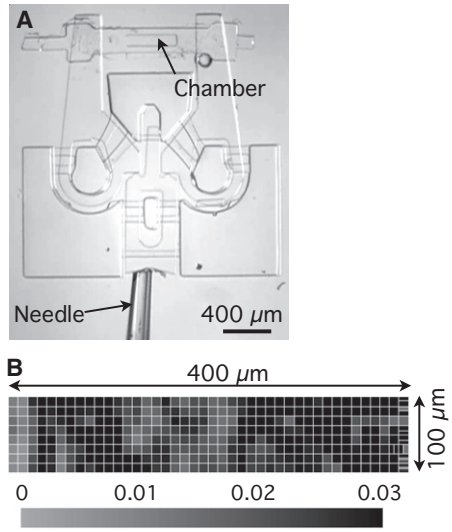

FIGURE 2 Microstretching device. (*A*) Overview of a device. By pushing a part of the device with a glass microneedle, the chamber is stretched in the horizontal direction. (*B*) Strain distribution of *A* when the magnitude of stretch in the entire microchamber is 0.26 (26% stretch). There is a roughly homogeneous strain field.

Evaluation of symmetrical distribution of GFP-myosin II and -ABD120k in response to the stretching of substratum

The cell area was divided into four portions by dotted lines (see Fig. 5 *B*). The lines were drawn from the centroid of the cell at angles of 45°, 135°, 225°, and 315° from the horizontal line. The areas 2 μm from the cell boundary in the four portions were defined as *a, b, c*, and *d*, respectively. F_a, F_b, F_c, and F_d are the maximum values of the fluorescence of GFP-myosin II or GFP-ABD120k in areas *a–d*, respectively. $F_i|F_j$, which is an index of the symmetrical distribution, is expressed as the larger of F_i and F_j divided by the smaller. When the distribution of myosin II or actin filaments is symmetrical in the *i* and *j* areas, the value should be 1. When it is asymmetrical, the value should be larger.

Evaluation of the relationship between pseudopod dynamics and GFP-myosin II localization in response to the stretching of substratum

To estimate the localization of myosin II in response to the stretching and its role of following pseudopod dynamics, two images were taken before and after four repeats of 20% stretching (Fig. 1, *D* and *E*). In the first of these images (Fig. 1 *D*), a dotted line was drawn from the centroid to a point on the boundary of a cell. On the dotted line, the distance from the centroid to the point was defined as l_1. The maximum value of GFP fluorescence in the area defined by the intersection of the dotted line and the orbital area 2 μm from the cell boundary (Fig. 1 *D*, *gray area*) was defined as F_1 (Fig. 1 *D*, *black bar*). In the second image (Fig. 1 *E*), a dotted line was drawn from the centroid before, not after, stretching in the same direction as in the first image. The distance between the centroid before stretching and the cell boundary was defined as l_2. F_2 (Fig. 1 *E*, *black bar*) was defined in the same manner as F_1.

Dotted lines were drawn from the centroid of the cell at angles of 0°, 45°, 135°, 180°, 225°, and 315° from the horizontal line (Fig. 1 *F*). The values of l_2/l_1 and F_2/F_1 were calculated for the six areas on the dotted

line (Fig. 1 *F, black bars*). When pseudopod expansion takes place in the area, the l_2/l_1 value should be >1. When myosin II localization takes place, the F_2/F_1 value should be >1.

RESULTS

Directional migration of wild-type cells in response to cyclic stretching of elastic substratum

Cyclic stretching stimuli were applied to wild-type cells by repeated stretching and relaxation of the substratum, in which the stretching ratio and the time cycle were 20% and 5 s, respectively. Trajectories of cell migrations (Fig. 3 *A*) and frequencies of migrating directions (Fig. 3 *C*) are shown. The cells tended to migrate perpendicular to the stretching direction (Fig. 3 *C*, *arrows*), whereas they migrated randomly in the absence of cyclic stretching (Fig. 3, *B* and *D*). The average $|\sin\theta|$ value (see Materials and Methods) calculated from Fig. 3 *C* (Fig. 3 *E*, *left*) was significantly higher than that from Fig. 3 *D* (Fig. 3 *E*, *right*), as was the case in a previous experiment using the cAR1/cAR3 chemoattractant cAMP receptor double-mutant cell line RI9 (16). These results indicate that *Dictyostelium* cells decide their migrating direction in response to forces from the substratum.

Myosin II is indispensable for directional migration of wild-type cells in response to cyclic stretching of elastic substratum

To clarify whether myosin II is a mediator of directional migration induced by the forces from the substratum, we observed the migration of *mhcA*$^-$ cells on the elastic substratum under cyclic stretching. The cells migrated randomly, although small fluctuations were seen (Fig. 4, *A* and *C*). There was no statistical difference in migration (Fig. 4 *E*), analyzed using the distribution of $|\sin\theta|$, between the case with cyclic stretching (Fig. 4, *A* and *C*) and that with no cyclic stretching (Fig. 4, *B* and *D*).

To test whether the cells sense a mechanical signal from the substratum through adhesion sites, we observed the migration of *sibA*$^-$ cells on the elastic substratum under cyclic stretching. SibA protein, similar to integrin beta protein, acts as an adhesion molecule in *Dictyostelium* (34). The cells tended to migrate perpendicular to the stretching direction (Fig. 4 *F*, *arrows*), whereas they migrated randomly in the absence of cyclic stretching (Fig. 4, *G* and *H*). The migration velocity was significantly decreased under cyclic stretching (Table 1). These results indicate that SibA-related adhesion is not required for transduction of the mechanical signal for directional migration, although it is required for maintaining migration velocity.

Next, localization of myosin II in response to the stretching of the elastic substratum was observed by dispersing *mhcA*$^-$ cells expressing GFP-myosin II on a fine microstretching device (36) (Fig. 2 *A*). After four repeats of 20% stretching, myosin II seemed to localize equally at the two edges of the stretched side in the cell (Fig. 5 *A*, *dotted ellipses*). The localization of myosin II was estimated quantitatively (Fig. 5, *B–F*; see Materials and Methods for details). Fluorescence intensities of GFP-myosin II in the stretching sides (Fig. 5, *C* and *D*, F_a and F_c) significantly increased after stretching (compare white columns of Fig. 5, *C* and *D*, $P = 0.001$ for F_a and 0.001 for F_c), whereas those in the other sides (Fig. 5, *C* and *D*, F_b and F_d) did not (compare gray columns of Fig. 5, *C* and *D*, $P = 0.49$ for F_b

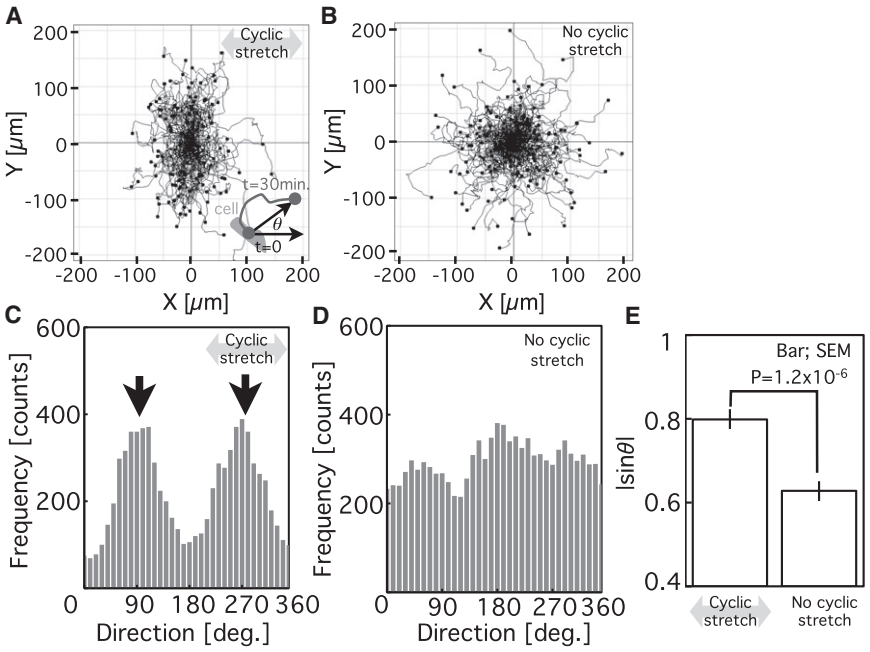

FIGURE 3 Crawling migrations of wild-type *Dictyostelium* cells on elastic substratum with cyclic stretching. Stretching ratio and time cycle were 20% and 5 s, respectively. (*A* and *B*) Trajectories of migrating cells under cyclic stretching in the horizontal (0°–180°) direction (*A*; $n = 120$ from five experiments) and under no cyclic stretching (*B*; $n = 161$ from six experiments). (*C* and *D*) Frequencies of migrating direction (θ) calculated from *A* and *B*, respectively. (*A*, *inset*) θ is defined as an angle between a horizontal line and a straight line connecting the starting and ending points, measured for each migrating cell during a single experiment for 30 min. (*E*) Average $|\sin\theta|$ values calculated from *C* and *D*. The $|\sin\theta|$ values on the substratum under cyclic stretching were significantly higher than those for no cyclic stretching ($P = 1.2 \times 10^{-6}$). Arrows in *C* indicate two peaks of frequencies at 90° and 270°. There is no significant peak in *D*.

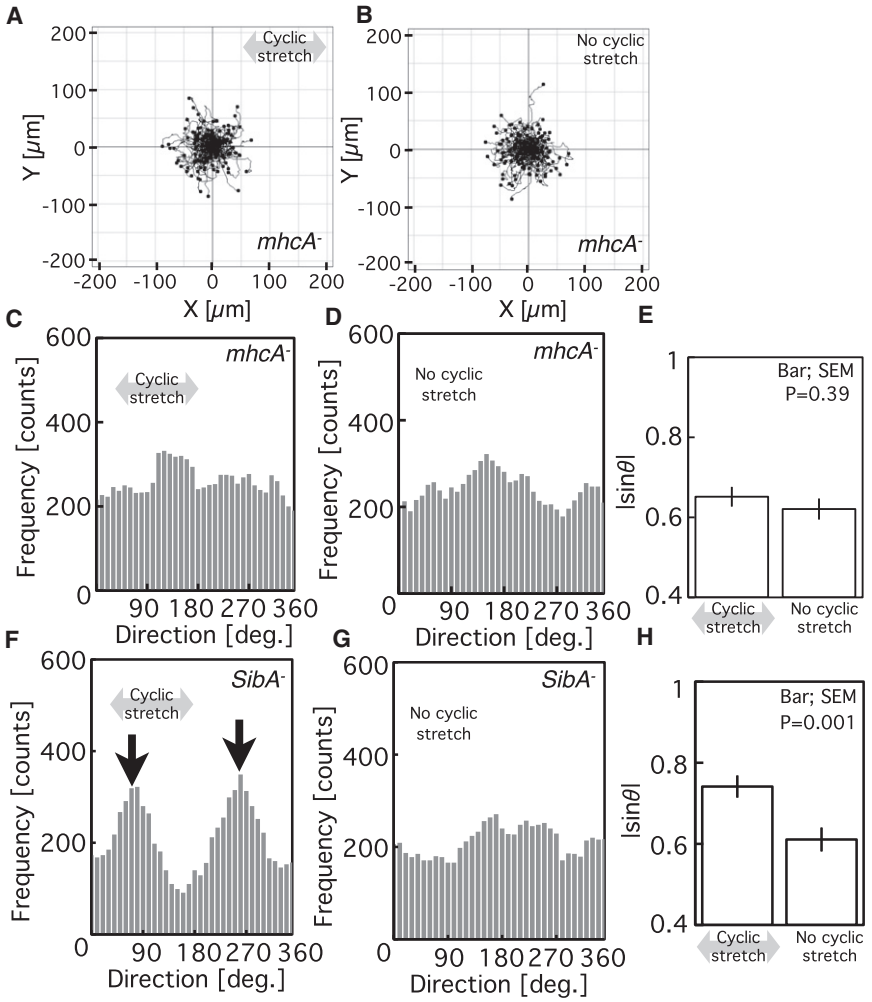

FIGURE 4 Crawling migrations of mutant cells on elastic substratum with cyclic stretching. Stretching ratio and time cycle were the same as in Fig. 3. (*A* and *B*) Trajectories of migrating *mhcA*$^-$ cells under cyclic stretching in the horizontal (0°–180°) direction (*A*; $n = 141$ from five experiments) and under no cyclic stretching (*B*; $n = 132$ from six experiments). (*C* and *D*) Frequencies of migrating direction (θ) calculated from *A* and *B*, respectively. (*E*) Average $|\sin\theta|$ values calculated from *C* and *D*. There is no significant difference between the stretching and no-stretching columns of $|\sin\theta|$ values ($P = 0.39$). (*F* and *G*) Frequencies of the migrating direction (θ) of *SibA*$^-$ cells under cyclic stretching in the horizontal (0°–180°) direction (*F*; $n = 114$ from six experiments) and under no cyclic stretching (*G*; $n = 116$ from six experiments). (*H*) Average $|\sin\theta|$ values calculated from *F* and *G*. There is a significant difference between the stretching and no-stretching columns of $|\sin\theta|$ values ($P = 0.001$).

and 0.06 for F_d). The ratio of the greater to the smaller fluorescence intensity of GFP-myosin II ($F_a|F_c$) in the stretching sides (Fig. 5 *B*, *a* and *c*) dramatically decreased after the stretching (Fig. 5, *E* and *F*, *left*), although that in the non-stretching sides ($F_b|F_d$) (Fig. 5 *B*, *b* and *d*) did not change (Fig. 5, *E* and *F*, *right*), indicating that the left-right

TABLE 1 Characteristics of migrations of all cell types on the substratum under cyclic stretching

		Wild-type	*mhcA*$^-$	*SibA*$^-$	3xALA	3xASP	E476K
Control	Velocity	7.1 ± 0.17	3.3 ± 0.08	5.6±0.31	10.5 ± 0.39	4.1 ± 0.11	6.5 ± 0.28
		0.38	0.03	0.001	0.88	0.26	0.89
	Velocity (X)	4.5 ± 0.11	1.9 ± 0.06	3.5 ± 0.21	6.6 ± 0.28	2.4 ± 0.08	4.0 ± 0.18
		0.55	0.11	0.61	0.97	0.09	0.66
	Velocity (Y)	4.4 ± 0.12	2.0 ± 0.06	3.4 ± 0.20	6.6 ± 0.24	2.6 ± 0.08	4.1 ± 0.19
	Directionality	0.32 ± 0.01	0.37 ± 0.01	0.35 ± 0.02	0.31 ± 0.01*[1]	0.37 ± 0.01	0.41 ± 0.02*[1]
		0.014	0.82	0.07	0.94	0.24	0.49
	n	161	132	116	117	128	83
Cyclic stretching	Velocity	7.4 ± 0.17	3.1 ± 0.07	4.4 ± 0.21	10.5 ± 0.38	4.3 ± 0.10	6.6 ± 0.36
	Velocity (X)	4.1 ± 0.11	1.8 ± 0.05	2.5 ± 0.13	5.9 ± 0.24	2.5 ± 0.07	3.8 ± 0.24
		1.1×10^{-7}	0.95	0.66	1.6×10^{-4}	3.7×10^{-4}	0.11
	Velocity (Y)	5.0 ± 0.13	1.8 ±0.05	2.9 ± 0.15	7.2 ± 0.27	2.8 ± 0.07	4.3 ± 0.23
	Directionality	0.37 ± 0.01	0.37 ± 0.02	0.40 ± 0.02	0.31 ± 0.01*[2]	0.35 ± 0.01	0.39 ± 0.02*[2]
	n	120	141	114	109	149	106

Velocity (X) and Velocity (Y) are the velocities of cells in the directions parallel and perpendicular to the stretching, respectively. *P* values for velocity and directionality between the Control and Cyclic stretching conditions are recorded below those values of Control. Those between Velocity (X) and Velocity (Y) in the Control and Cyclic stretching conditions are recorded below the Velocity (X) values. Some other statistical tests were performed (*1 and *2). *P* values of *1 and *2 are 1.5×10^{-4} and 9.7×10^{-4}, respectively.

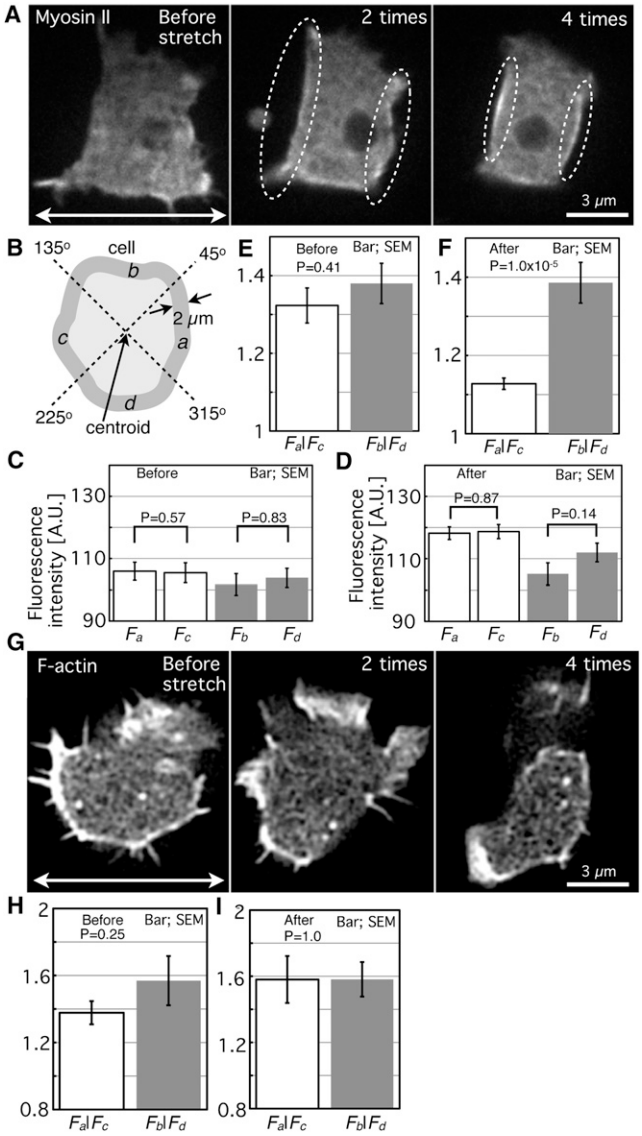

FIGURE 5 Myosin II localization caused by stretching of the substratum. (*A*) Typical localizations of GFP-myosin II by 20% stretching of the substratum using the device featured in Fig. 2 *A*, shown before stretching (*left*), after two stretches (*center*), and after four stretches (*right*). The *mhcA*$^-$ cells expressing GFP-myosin II were dispersed in the chamber of the device. The stretching directions are indicated by the double-headed arrow in the left panel. Localizations of GFP-myosin II were bilateral in the horizontal direction after two stretches (*dotted ellipses*) and became clearer after four stretches. (*B–F*) Evaluation of GFP-myosin II localization. (*B*) The cell area was divided into four portions by dotted lines. The areas 2 μm from the cell boundary in the four portions were defined as *a, b, c*, and *d*. F_a, F_b, F_c, and F_d are the maximal fluorescence values for GFP-myosin II in *a–d*, respectively. $F_i|F_j$ is expressed as the larger of F_i and F_j divided by the smaller. (*C*) F_a, F_b, F_c, and F_d before stretching. There was no significant difference between F_a and F_c ($n = 62$, $P = 0.57$), and F_b and F_d ($n = 62$, $P = 0.83$). (D) F_a, F_b, F_c, and F_d after four stretches. There was no significant difference between F_a and F_c ($n = 53$, $P = 0.87$), and F_b and F_d ($n = 53$, $P = 0.14$). F_a and F_c in *D* are significantly larger than the corresponding values in *C* ($P = 0.001$ for F_a and 0.001 for F_c), although there is no significant difference in F_b and F_d between *C* and *D* ($P = 0.49$ for F_b and 0.06 for F_d). (*E*) $F_a|F_c$ and $F_b|F_d$ before stretching. There was no significant difference between $F_a|F_c$ and $F_b|F_d$ ($P = 0.41$). (*F*) $F_a|F_c$ and $F_b|F_d$ after four stretches. $F_a|F_c$ significantly decreased, although $F_b|F_d$ did not change ($P = 1 \times 10^{-5}$). (*G*) Typical localizations of GFP-ABD120k by 20% stretching of the substratum using the device shown in Fig. 2 *A*. Actin meshwork was shown as fluorescence of GFP-ABD120k in midcell. Actin filaments in the meshwork did not align in any direction, even after four repeats of stretching. In the boundary of the cell, localization of actin filaments was shown. (*H* and *I*) Evaluation of localizations of GFP-ABD120k before stretching (*H*; $n = 29$) and after four stretches (*I*; $n = 21$).

symmetrical forces induce the same symmetrical localization of myosin II.

Dictyostelium cells have a dense actin meshwork instead of thick, straight filaments like stress fibers (17,18). To clarify whether not only myosin II but also actin meshwork responds to the forces from the substratum, we next observed the distribution of actin filaments in the meshwork before and after four repeats of 20% stretching by dispersing wild-type cells expressing GFP-ABD120k on the device shown in Fig. 2 *A* (Fig. 5 *G*). In the middle of the cell, actin filaments did not show alignment in a particular direction, even after four repeats of stretching.

Our next step was to estimate the localization of actin filaments on the boundary of the cell (Fig. 5, *H* and *I*), which was done in the same way as for myosin II (Fig. 5 *E* and *F*). There was no significant difference in the ratio of the greater to the smaller fluorescence intensity of GFP-ABD120k between the two stretching sides (Fig. 5 *B*, *a* and *c*) before (Fig. 5 *H*, $F_a|F_c$) and after (Fig. 5 *I*, $F_a|F_c$) four repeats of 20% stretching. In the nonstretching side, too, there was no significant difference before (Fig. 5 *H*, $F_b|F_d$) and after (Fig. 5 *I*, $F_b|F_d$) the stretching, indicating that localization of actin filaments has no relation to the stretching.

Assembly of thick filaments rather than contraction of actomyosin is required for directional migration in response to cyclic stretching

To determine what function of myosin II is essential for directional migration in response to cyclic stretching, three types of *mhcA*$^-$ cells were used in the following experiments. The first was *mhcA*$^-$ cells expressing GFP-3xALA myosin II, a myosin II that constitutively assembles into filaments; the second was *mhcA*$^-$ cells expressing GFP-3xASP myosin II, a myosin II that cannot form thick filaments; and the third was *mhcA*$^-$ cells expressing GFP-E476K myosin II, a myosin II that cannot hydrolyze ATP. These three types of *mhcA*$^-$ cell are referred to as 3xALA, 3xASP, and E476K cells, respectively.

Localization of myosin II variants in response to stretching of the elastic substratum were observed by dispersing *mhcA*$^-$ cells on the device pictured in Fig. 2 *A* (Fig. 6). After four repeats of 20% stretching, GFP-3xALA and GFP-E476K myosin II localized equally at the two edges of the stretched sides in the cell (Fig. 6, *A* and *C* (*dotted ellipses*),

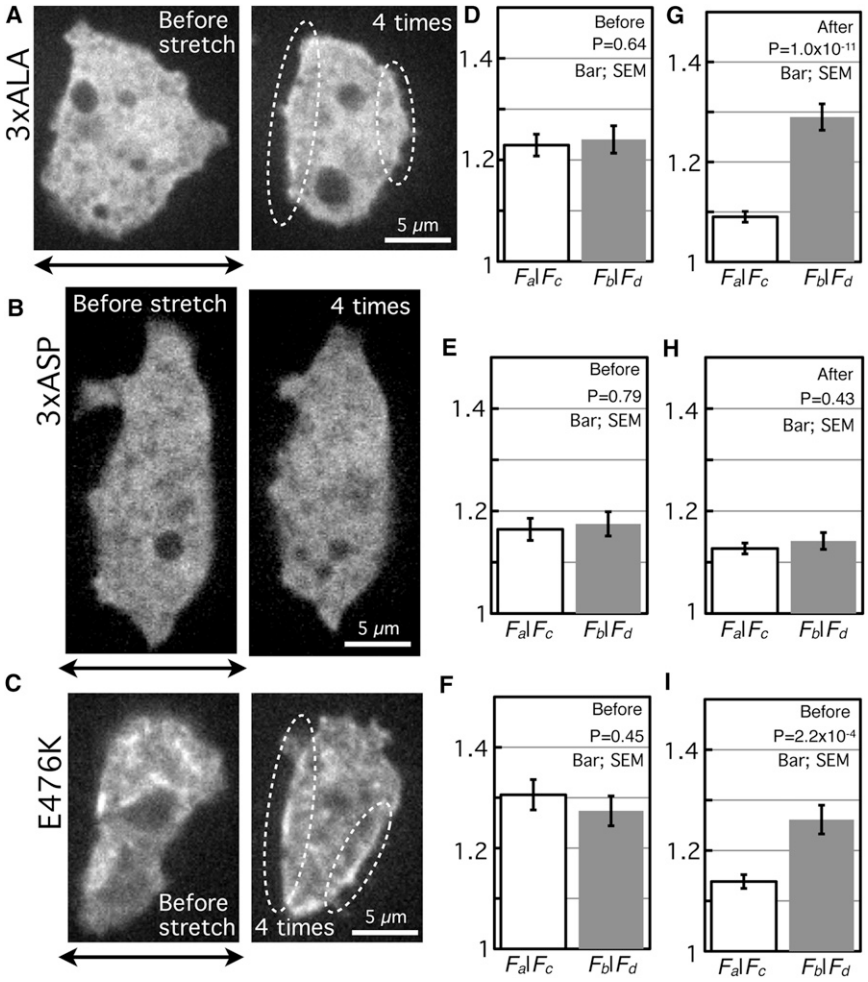

FIGURE 6 Localization of myosin II variants caused by stretching of the substratum using the device shown in Fig. 2 *A*. (*A–C*) Typical localization of GFP-3xALA, GFP-3xASP, and GFP-E476K myosin II in *mhcA*$^-$ cells by 20% stretching of the substratum, shown before stretching (*left*) and after four repeats of stretching (*right*). The stretching directions are indicated by double-headed arrows under the left images. Localizations of GFP-3xALA and -E476K myosin II were bilateral in the horizontal direction after four repeats of stretching (*dotted ellipses*), although uniform localization of GFP-3xASP myosin II was not changed by the stretching. (*D–I*) Evaluation of localizations of GFP-myosin II variants. Data were calculated in the same manner as for Fig. 5, *E* and *F*. (*D–F*) GFP-3xALA, GFP-3xASP, and GFP-E476K myosin II, respectively, before stretching. In all variants, there is no significant difference between $F_a|F_c$ and $F_b|F_d$ ($n = 144$ (GFP-3xALA), 160 (GFP-3xASP), and 130 (GFP-E476K), $P > 0.1$). (*G–I*) GFP-3xALA, GFP-3xASP, and GFP-E476K myosin II, respectively, after four repeats of stretching. In the case of GFP-3xALA and GFP-E476K myosin II, $F_a|F_c$ is significantly smaller than $F_b|F_d$ ($n = 142$ (GFP-3xALA) and 101 (GFP-E476K), $P < 0.01$). There is no significant difference in $F_a|F_c$ and $F_b|F_d$ in GFP-3xASP myosin II.

and *D*, *F*, *G*, and *I* (*open columns*)). However, the distribution of GFP-3xASP myosin II was not affected (Fig. 6, *B*, *E*, and *H*).

In cell migrations, 3xALA and E476K cells migrated perpendicular to the stretching direction on the elastic substratum under cyclic stretching (Fig. 7, *A* and *C*, *arrows*), whereas they migrated randomly in the absence of cyclic stretching (Fig. 7, *D* and *F*). Average $|\sin\theta|$ values calculated from Fig. 7, *A* and *C* (Fig. 7, *G* and *I*, *right columns*), were significantly higher than those from Fig. 7, *D* and *F* (Fig. 7, *G* and *I*, *left columns*), as was the case for wild-type cells (Fig. 3). On the other hand, 3xASP cells migrated randomly on the elastic substratum under cyclic stretching (Fig. 7 *B*). There was no statistical difference in migration (Fig. 7 *H*) between the case with cyclic stretching (Fig. 7 *B*) and that with no cyclic stretching (Fig. 7 *E*), as was the case for *mhcA*$^-$ cells (Fig. 4 *E*).

Thus, it is tentatively summarized that 1), only the filamentous myosin II can respond to forces; 2), localization of myosin II takes place in response to external forces; 3), no contraction of actomyosin is necessary for the localization; and 4), directional migration requires not contraction of actomyosin but localization of myosin II filaments in response to cyclic stretching. Characteristics of migration of all cell types on the substratum under cyclic stretching are summarized in Table 1. Statistical tests were performed between Velocity (X) and Velocity (Y) both under cyclic stretching and under no cyclic stretching. Under cyclic stretching, the velocities of cell types other than *mhcA*$^-$ in the direction perpendicular to the stretching were greater than those in the direction parallel to the stretching, although there was no significant difference in *SibA*$^-$ and E476K cells. Directionality was also compared statistically between cells under cyclic stretching and those under no cyclic stretching. In all cell types, directionality was <0.5 in both the presence and absence of cyclic stretching. *P* values for each cell type under cyclic stretching and in the absence of cyclic stretching are >0.01.

Localization of myosin II prevents pseudopod expansion without contraction as actomyosin

To test how localization of myosin II affects cell migration without contraction as actomyosin, we estimated the

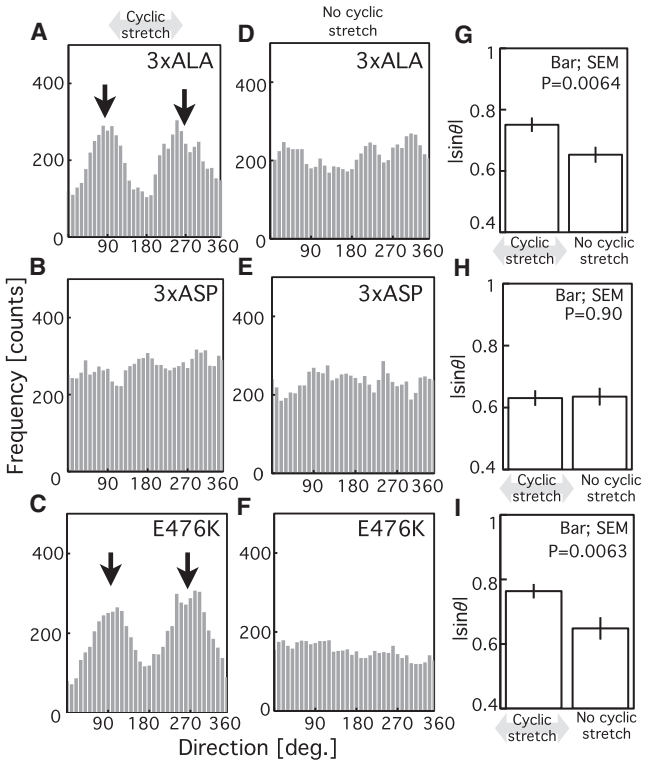

FIGURE 7 Crawling migrations of *mhcA*$^-$ cells expressing GFP-myosin II variants on elastic substratum with cyclic stretching. Stretching ratio and time cycle were the same as in Fig. 3. (*A–C*) Frequencies of the migrating direction (θ) of 3xALA cells (*A*; $n = 109$ from six experiments), 3xASP cells (*B*; $n = 149$ from eight experiments), and E476K cells (*C*; $n = 106$ from six experiments) under cyclic stretching in the horizontal (0°–180°) direction. Arrows in *A* and *C* indicate two peaks at 90° and 270°. (*D–F*) Frequencies of migrating direction (θ) of 3xALA cells (*D*; $n = 119$ from eight experiments), 3xASP cells (*E*; $n = 128$ from eight experiments), and E476K cells (*F;* $n = 83$ from five experiments) in the absence of cyclic stretching. (*G–I*) Average $|\sin\theta|$ values. The values of the left and right columns in each graph were calculated from the migrations under cyclic stretching (*A–C*) and with no cyclic stretching in the horizontal (0°–180°) direction (*D–F*), respectively. In 3xALA and E476K cells, the $|\sin\theta|$ values were significantly higher in response to cyclic stretching than in the absence of stretching (*G* and *I*, $P < 0.01$).

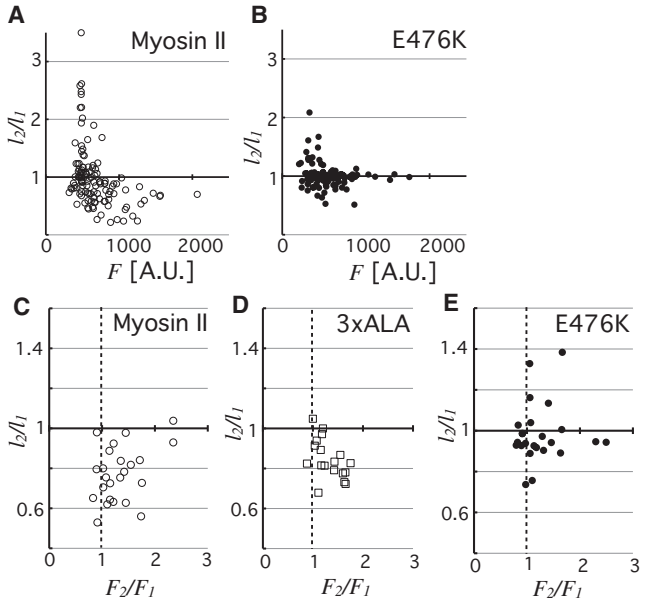

FIGURE 8 Localization of myosin II and pseudopod dynamics that follow. (*A* and *B*) Freely migrating *mhcA*$^-$ cells expressing GFP-myosin II (*A*) and E476K cells (*B*) on a coverslip. *F* refers to spontaneous localization of myosin II in freely migrating cells. The value l_2/l_1 means the contraction or expansion of pseudopodia. (*C–E*) The *mhcA*$^-$ cells expressing GFP-myosin II (*C*), 3xALA (*D*), and E476K cells (*E*) under cyclic stretching using the device shown in Fig. 2 *A*. F_2/F_1 means localization of myosin II in response to the four repeats of stretching of substratum. Dotted lines in *C–E* are where $F_2/F_1 = 1$.

relationship between pseudopod movements and localization of E476K myosin II in cells both on a coverslip and on an elastic substratum with cyclic stretching.

First, from the sequential images of free migration of *mhcA*$^-$ cells expressing GFP-myosin II or GFP-E476K myosin II on a coverslip, the values of *F*, l_1, and l_2 in Fig. 1, *A* and *B* (see Materials and Methods for details), were measured along 12 directions at intervals of 30° (Fig. 1 *C*). *F* reflects the spontaneous localization of myosin II in freely migrating cells. The value l_2/l_1 reflects the contraction or expansion of pseudopodia. When l_2/l_1 was >1, the pseudopod expanded, and when it was <1, the pseudopod contracted. In the case of *mhcA*$^-$ cells expressing GFP-myosin II (see Fig. 8 *A*), the l_2/l_1 values at high *F* values were <1, indicating that spontaneous localization of myosin II induced contraction of the pseudopod. On the other hand, in the case of E476K cells (see Fig. 8 *B*), although the l_2/l_1 values at low *F* values were >1, as is the case for *mhcA*$^-$ cells expressing GFP-myosin II, those at high *F* values were almost 1, indicating that the spontaneous localization of E476K myosin II did not induce retraction of the pseudopodia but prevented their expansion.

The next step was to estimate the role of E476K myosin II under cyclic stretching of the substratum from the data presented in Figs. 5 and 6. In these experiments, the values of F_1, F_2, l_1, and l_2 in Fig. 1, *D* and *E* (see Materials and Methods for details), were measured in the stretching direction (Fig. 1 *F*, *black bars*). F_2/F_1 reflects localization of myosin II in response to the four repeats of stretching of the substratum. The value l_2/l_1 reflects the contraction or expansion of pseudopodia. In all cases (see Fig. 8, *C*, *D*, and *E*), the F_2/F_1 values were >1, indicating the localization of myosin II and 3xALA and E476K myosin II at the stretching side in response to the stretching. On the other hand, although the l_2/l_1 values in *mhcA*$^-$ cells expressing GFP-myosin II and 3xALA cells (see Fig. 8, *C* and *D*) were <1, those in E476K cells ranged around 1(see Fig. 8 *E*). These results indicate that localization of myosin II and 3xALA myosin II at the stretching sides of the cell induce retraction of the pseudopodia there and make the cell shape short at the sides, whereas localization of E476K myosin II did not induce retraction of the

pseudopodia but prevented their expansion, as was the case of freely migrating E476K cells.

DISCUSSION

In response to the cyclic stretching of the elastic substratum, intracellular stress fibers in fibroblasts and in endothelial, osteosarcoma, and smooth muscle cells are rearranged perpendicular to the stretching direction (9–15). *Dictyostelium* cells have a dense actin meshwork instead of stress fibers (17,18). In the middle of the cell, actin filaments did not show alignment in a particular direction (Fig. 5 *G*), whereas the distribution of actin filaments on the boundary of the cell continuously changed, even during cyclic stretching (Fig. 5 *G*), and was independent of the stretching (Fig. 5, *H* and *I*). Alternatively, myosin II localized equally at the two edges of the stretched side in the cell (Fig. 5, *E* and *F*). The molecular dynamics in *Dictyostelium* cells in response to stretching differs from that in mammalian cells such as fibroblasts and endothelial cells. *Dictyostelium* cells are known to be a kind of fast-moving cell. The migrating speed of *Dictyostelium* cells (~10 μm/min) (16) is much faster than that of fibroblasts (<1 μm/min) (37). Migration of other fast-moving cells, such as keratocytes and leukocytes, on elastic substratum with cyclic stretching may be one of the interesting issues for future investigation.

In fibroblasts, it is widely thought that a mechanical signal from the substratum is transmitted through their adhesion sites as deformations of focal adhesion proteins, such as p130Cas (37–39). To test whether *Dictyostelium* cells sense a mechanical signal from the substratum through adhesion sites, as in the case of fibroblasts, we observed the migration of *SibA*$^-$ cells on the elastic substratum under cyclic stretching. The cells could attach to the surface of the substratum while the adhesiveness decreased and tended to migrate perpendicular to the stretching direction (Fig. 4 *F*), indicating that SibA protein is not necessarily required for adhesion to the substratum, nor is itrequired for mechanosensing of *Dictyostelium* cells. However, it should contribute to stable migration, because the migration velocity of *SibA*$^-$ cells significantly decreased under cyclic stretching ($P = 0.001$ in Table 1).

Dictyostelium cells show straight migration to the chemoattractant, cAMP (40), or cathode under electric fields (41). The directionalities of those cells reach almost 1, whereas directionalities of all the cell types shown in Table 1 under cyclic stretching were between 0.31 and 0.41. These values are much smaller than those of chemotactic or galvanotactic cells. Moreover, there was no significant difference in directionality between the cyclic stretching condition and no stretching. Even under no cyclic stretching, cells can migrate, although the direction is random. Those cells may make their polarity for migration in response to the reaction forces from the substratum of their own tractions. The polarity generation for migration utilizing the force from the substratum may be one of the most fundamental mechanisms, and chemotaxis and galvanotaxis are highly sophisticated ones.

How does myosin II localize in response to the stretching of the elastic substratum? There are several possibilities: 1), mechanical signal from the substratum is transmitted through their adhesion sites as deformations of focal adhesion proteins other than SibA; 2), mechanical signal induces activation of unidentified mechanosensitive channels; or 3), actin filaments are deformed. Deformation of actin filaments is a possible candidate to induce the myosin II localization, because actin meshwork is required for myosin II localization (42,43), just as the affinity of cofilin to the actin is modulated by the deformation of actin filaments (44). Recently, we showed that stretching actin filaments within *Dictyostelium* cells enhances their affinity for myosin II (43). This situation is just as valid for the localization of myosin II during cytokinesis. The *mhcA*$^-$ *Dictyostelium* cells perform cytokinesis on adhesive substratum, although they cannot do so under nonadhesive conditions (45,46). During cytokinesis, GFP-E476K myosin II localizes in the equatorial region, where the strain of the cell cortex should be maximal (32). Sucking of the cell using a micropipette also localizes myosin II at the tip of the sucked cell lobe (23,24). These observations suggest that myosin II localizes in response to stretching of the cell, although it is not possible in this study to distinguish whether stretching or relaxation of the substratum induces localization of myosin II.

Localization of GFP-E476K myosin II and perpendicular migration of E476K cells on elastic substratum under cyclic stretching indicate that it is not contraction of actomyosin but assembly of thick filaments that is required for both localization and perpendicular migration in response to cyclic stretching (Figs. 6 *C* and 7 *C*). The directionality of E476K cells is larger than that of 3xALA, not only under cyclic stretching but also in the absence of cyclic stretching (*1 and *2 in Table 1). These results also indicate that contraction of actomyosin is not necessarily required for directional migration. The defect in E476K myosin has to do with the hydrolysis of ATP (33). In the presence of ATP, therefore, most of the heads of the mutants bind ATP and form weak bindings with actin. The probability of binding of an E476K myosin II monomer to actin is low. That of binding of thick filaments should be high enough to keep binding to the actin filaments not only in migrating cells in this study but also in dividing cells (32). Localized E476K myosin II filaments prevent elongation of pseudopodia without contraction of actomyosin (Fig. 8). Localized thick filaments of myosin II may induce cross-linking of actin filaments and stabilize the cortex of the cell. This hypothesis agrees well with earlier findings in *Dictyostelium* cells, in which cells lacking myosin II or components that regulate its assembly were unable to suppress lateral

pseudopodia (25,26,47). The detailed mechanism is an interesting topic for future study.

We thank Dr. T. Q. Uyeda (AIST, Tsukuba, Japan) for the kind gifts of the GFP-ABD120k, GFP-myosin II, GFP-3xALA myosin II, GFP-3xASP myosin II, and GFP-E476K myosin II expression plasmids, Dr. D. A. Knecht (University of Connecticut, Storrs, CT) for permission to use the GFP-ABD120k expression plasmid, Dr. S. Yumura (Yamaguchi University, Yamaguchi, Japan) for support of the preliminary experiments, and Dr. M. Kikuyama (Niigata University, Niigata, Japan) for critical reading of the manuscript.

Y.I. was supported by Grant-in-Aid 23111519 and The Yamaguchi University Strategic Program for Fostering Research Activities.

REFERENCES

1. Chien, S. 2008. Effects of disturbed flow on endothelial cells. *Ann. Biomed. Eng.* 36:554–562.
2. Ricci, A. J., B. Kachar, …, S. M. Van Netten. 2006. Mechano-electrical transduction: new insights into old ideas. *J. Membr. Biol.* 209:71–88.
3. Giannone, G., and M. P. Sheetz. 2006. Substrate rigidity and force define form through tyrosine phosphatase and kinase pathways. *Trends Cell Biol.* 16:213–223.
4. Vogel, V., and M. Sheetz. 2006. Local force and geometry sensing regulate cell functions. *Nat. Rev. Mol. Cell Biol.* 7:265–275.
5. Naruse, K., T. Yamada, …, M. Sokabe. 1998. Pp125FAK is required for stretch dependent morphological response of endothelial cells. *Oncogene.* 17:455–463.
6. Naruse, K., T. Yamada, and M. Sokabe. 1998. Involvement of SA channels in orienting response of cultured endothelial cells to cyclic stretch. *Am. J. Physiol.* 274:H1532–H1538.
7. Crosby, L. M., C. Luellen, …, C. M. Waters. 2011. Balance of life and death in alveolar epithelial type II cells: proliferation, apoptosis, and the effects of cyclic stretch on wound healing. *Am. J. Physiol. Lung Cell. Mol. Physiol.* 301:L536–L546.
8. Desai, L. P., S. R. White, and C. M. Waters. 2010. Cyclic mechanical stretch decreases cell migration by inhibiting phosphatidylinositol 3-kinase- and focal adhesion kinase-mediated JNK1 activation. *J. Biol. Chem.* 285:4511–4519.
9. Birukov, K. G., J. R. Jacobson, …, J. G. Garcia. 2003. Magnitude-dependent regulation of pulmonary endothelial cell barrier function by cyclic stretch. *Am. J. Physiol. Lung Cell. Mol. Physiol.* 285: L785–L797.
10. Kaunas, R., P. Nguyen, …, S. Chien. 2005. Cooperative effects of Rho and mechanical stretch on stress fiber organization. *Proc. Natl. Acad. Sci. USA.* 102:15895–15900.
11. Tondon, A., H.-J. Hsu, and R. Kaunas. 2012. Dependence of cyclic stretch-induced stress fiber reorientation on stretch waveform. *J. Biomech.* 45:728–735.
12. Lee, C.-F., C. Haase, …, R. Kaunas. 2010. Cyclic stretch-induced stress fiber dynamics: dependence on strain rate, Rho-kinase and MLCK. *Biochem. Biophys. Res. Commun.* 401:344–349.
13. Zhao, L., C. Sang, …, F. Zhuang. 2011. Effects of stress fiber contractility on uniaxial stretch guiding mitosis orientation and stress fiber alignment. *J. Biomech.* 44:2388–2394.
14. Sato, K., T. Adachi, …, Y. Tomita. 2005. Quantitative evaluation of threshold fiber strain that induces reorganization of cytoskeletal actin fiber structure in osteoblastic cells. *J. Biomech.* 38:1895–1901.
15. Morioka, M., H. Parameswaran, …, S. Ito. 2011. Microtubule dynamics regulate cyclic stretch-induced cell alignment in human airway smooth muscle cells. *PLoS ONE.* 6:e26384.
16. Iwadate, Y., and S. Yumura. 2009. Cyclic stretch of the substratum using a shape-memory alloy induces directional migration in *Dictyostelium* cells. *Biotechniques.* 47:757–767.
17. Bretschneider, T., S. Diez, …, G. Gerisch. 2004. Dynamic actin patterns and Arp2/3 assembly at the substrate-attached surface of motile cells. *Curr. Biol.* 14:1–10.
18. Iwadate, Y., and S. Yumura. 2008. Molecular dynamics and forces of a motile cell simultaneously visualized by TIRF and force microscopies. *Biotechniques.* 44:739–750.
19. Svitkina, T. M., A. B. Verkhovsky, …, G. G. Borisy. 1997. Analysis of the actin-myosin II system in fish epidermal keratocytes: mechanism of cell body translocation. *J. Cell Biol.* 139:397–415.
20. Wang, Y. L. 1985. Exchange of actin subunits at the leading edge of living fibroblasts: possible role of treadmilling. *J. Cell Biol.* 101:597–602.
21. Jay, P. Y., P. A. Pham, …, E. L. Elson. 1995. A mechanical function of myosin II in cell motility. *J. Cell Sci.* 108:387–393.
22. Chen, W. T. 1981. Mechanism of retraction of the trailing edge during fibroblast movement. *J. Cell Biol.* 90:187–200.
23. Merkel, R., R. Simson, …, E. Sackmann. 2000. A micromechanic study of cell polarity and plasma membrane cell body coupling in *Dictyostelium*. *Biophys. J.* 79:707–719.
24. Ren, Y., J. C. Effler, …, D. N. Robinson. 2009. Mechanosensing through cooperative interactions between myosin II and the actin crosslinker cortexillin I. *Curr. Biol.* 19:1421–1428.
25. Chung, C. Y., G. Potikyan, and R. A. Firtel. 2001. Control of cell polarity and chemotaxis by Akt/PKB and PI3 kinase through the regulation of PAKa. *Mol. Cell.* 7:937–947.
26. Wessels, D., D. R. Soll, …, J. Spudich. 1988. Cell motility and chemotaxis in *Dictyostelium* amebae lacking myosin heavy chain. *Dev. Biol.* 128:164–177.
27. Clow, P. A., and J. G. McNally. 1999. In vivo observations of myosin II dynamics support a role in rear retraction. *Mol. Biol. Cell.* 10:1309–1323.
28. Eliott, S., G. H. Joss, …, K. L. Williams. 1993. Patterns in *Dictyostelium* discoideum: the role of myosin II in the transition from the unicellular to the multicellular phase. *J. Cell Sci.* 104:457–466.
29. Iwadate, Y., and S. Yumura. 2008. Actin-based propulsive forces and myosin-II-based contractile forces in migrating *Dictyostelium* cells. *J. Cell Sci.* 121:1314–1324.
30. Pang, K. M., E. Lee, and D. A. Knecht. 1998. Use of a fusion protein between GFP and an actin-binding domain to visualize transient filamentous-actin structures. *Curr. Biol.* 8:405–408.
31. Egelhoff, T. T., R. J. Lee, and J. A. Spudich. 1993. *Dictyostelium* myosin heavy chain phosphorylation sites regulate myosin filament assembly and localization in vivo. *Cell.* 75:363–371.
32. Yumura, S., and T. Q. Uyeda. 1997. Transport of myosin II to the equatorial region without its own motor activity in mitotic *Dictyostelium* cells. *Mol. Biol. Cell.* 8:2089–2099.
33. Ruppel, K. M., and J. A. Spudich. 1996. Structure-function studies of the myosin motor domain: importance of the 50-kDa cleft. *Mol. Biol. Cell.* 7:1123–1136.
34. Cornillon, S., L. Gebbie, …, P. Cosson. 2006. An adhesion molecule in free-living *Dictyostelium* amoebae with integrin beta features. *EMBO Rep.* 7:617–621.
35. Tsujioka, M., S. Yumura, …, S. Yonemura. 2012. Talin couples the actomyosin cortex to the plasma membrane during rear retraction and cytokinesis. *Proc. Natl. Acad. Sci. USA.* 109:12992–12997.
36. Sato, K., S. Kamada, and K. Minami. 2010. Development of micro-stretching device to evaluate cell membrane strain field around sensing point of mechanical stimuli. *Int. J. Mech. Sci.* 52:251–256.
37. Wang, H. B., M. Dembo, …, Y. Wang. 2001. Focal adhesion kinase is involved in mechanosensing during fibroblast migration. *Proc. Natl. Acad. Sci. USA.* 98:11295–11300.

38. Jiang, G., A. H. Huang, …, M. P. Sheetz. 2006. Rigidity sensing at the leading edge through $\alpha_v\beta_3$ integrins and RPTPα. *Biophys. J.* 90:1804–1809.

39. Sawada, Y., M. Tamada, …, M. P. Sheetz. 2006. Force sensing by mechanical extension of the Src family kinase substrate p130Cas. *Cell.* 127:1015–1026.

40. Park, K. C., F. Rivero, …, R. A. Firtel. 2004. Rac regulation of chemotaxis and morphogenesis in *Dictyostelium*. *EMBO J.* 23:4177–4189.

41. Sato, M. J., H. Kuwayama, …, M. Ueda. 2009. Switching direction in electric-signal-induced cell migration by cyclic guanosine monophosphate and phosphatidylinositol signaling. *Proc. Natl. Acad. Sci. USA.* 106:6667–6672.

42. Bosgraaf, L., and P. J. M. van Haastert. 2006. The regulation of myosin II in *Dictyostelium*. *Eur. J. Cell Biol.* 85:969–979.

43. Uyeda, T. Q. P., Y. Iwadate, …, S. Yumura. 2011. Stretching actin filaments within cells enhances their affinity for the myosin II motor domain. *PLoS ONE.* 6:e26200.

44. Galkin, V. E., A. Orlova, …, E. H. Egelman. 2001. Actin depolymerizing factor stabilizes an existing state of F-actin and can change the tilt of F-actin subunits. *J. Cell Biol.* 153:75–86.

45. Zang, J. H., G. Cavet, …, J. A. Spudich. 1997. On the role of myosin-II in cytokinesis: division of *Dictyostelium* cells under adhesive and nonadhesive conditions. *Mol. Biol. Cell.* 8:2617–2629.

46. De Lozanne, A., and J. A. Spudich. 1987. Disruption of the *Dictyostelium* myosin heavy chain gene by homologous recombination. *Science.* 236:1086–1091.

47. Parent, C. A. 2004. Making all the right moves: chemotaxis in neutrophils and *Dictyostelium*. *Curr. Opin. Cell Biol.* 16:4–13.